

Landau-Zener quantum tunneling in disordered nanomagnets

V.G. Benza

Dipartimento di Fisica e Matematica, Universita' dell'Insubria,

Como, I.N.F.M., sezione di Como, Italy

C.M. Canali

Division of Physics, Department of Chemistry and Biomedical Sciences,

Kalmar University, 391 82 Kalmar, Sweden

G. Strini

Dipartimento di Fisica, Universita' di Milano, Milano, Italy

(Dated: November 13, 2018)

Abstract

We study Landau-Zener macroscopic quantum transitions in ferromagnetic metal nanoparticles containing on the order of 100 atoms. The model that we consider is described by an effective giant-spin Hamiltonian, with a coupling to a random transverse magnetic field mimicking the effect of quasiparticle excitations and structural disorder on the gap structure of the spin collective modes. We find different types of time evolutions depending on the interplay between the disorder in the transverse field and the initial conditions of the system. In the absence of disorder, if the system starts from a low-energy state, there is one main coherent quantum tunneling event where the initial-state amplitude is completely depleted in favor of a few discrete states, with nearby spin quantum numbers; when starting from the highest excited state, we observe complete inversion of the magnetization through a peculiar “backward cascade evolution”. In the random case, the disorder-averaged transition probability for a low-energy initial state becomes a smooth distribution, which is nevertheless still sharply peaked around one of the transitions present in the disorder-free case. On the other hand, the coherent backward cascade phenomenon turns into a damped cascade with frustrated magnetic inversion.

I. INTRODUCTION

Ferromagnetic transition metal nanoparticles[1, 2, 3] and molecular nanomagnets [4, 5] have been actively studied over the past decade and are presently the subject of strong interest and intense investigation. So far, interest in ferromagnetic transition metal nanoparticles has been mainly motivated by their relevance to high-performance information storage technology and spin electronics[6, 7]. Recently a lot of progress has been made in characterizing the physical properties of individual ferromagnetic nanoparticles, such as their magnetic anisotropy[8]. However, reproducible and controlled fabrication is still difficult and the understanding of their classical dynamics is still not a fully solved problem[9]. Molecular magnets, on the other hand, are relatively simple and well characterized magnetic systems that offer the possibility of studying a rich interplay of classical and *quantum* magnetic phenomena[5]. Among the latter, the coherent quantum tunneling of the magnetization in molecular magnets is one of the most fascinating phenomena[10, 11] [45]. Thermally activated quantum tunneling of the magnetization (QTM) has been observed experimentally in molecular magnets such as Mn₁₂[12, 13] and Fe₈[14]. In these experiments, a sequence of discrete steps in the magnetic hysteresis curve provides a direct evidence of resonant coherent quantum tunneling between collective spin quantum states. For Fe₈, there is strong evidence that at low temperatures (below 360 mK) the system enters a quantum regime where the reversal of the magnetization is caused by a pure tunneling mechanism[14, 15]. The occurrence of macroscopic QTM has also been investigated in ferromagnetic nanoparticles. Despite the effective spin of a few nanometer particle is typically several orders of magnitude larger than the spin of a molecular magnet (where $S = 10$) earlier theoretical work[10] predicts that QTM in these systems should be possible by applying an external field close to the classical switching field in the direction opposite to the magnetization. On the experimental front, some evidence of quantum effects was found in switching field measurements in ferrimagnetic BaFeO nanoparticles[16]. However, it is fair to say that experimental proof for QTM in single-domain nanoparticles is still a controversial issue. Unambiguous evidence of QTM can only be provided by the observation of level quantization of the collective spin states like in the case of molecular magnets. For BaFeO nanoparticles with $S = 10^5$, the magnetic field steps associated with such quantizations should be of the order of a $\Delta H = H_a/2S \approx 0.002$ mT (where H_a is the anisotropy field), which is too small even

for the most sensitive and sophisticated magnetic measurement techniques, such as the new microSQUID set-up used in Ref. 8. It seems clear that new experiments in this direction, presently underway, should focus on nanoparticles containing on the order of a few hundred atoms. In discussing ferromagnetic nanoparticles it is important to draw a clear distinction between insulating particles, for which the only low-energy degree of freedom is the collective spin-orientation, and metal nanoparticles, which have discrete particle-hole excitations in addition. The common practice of modeling a magnetic particle by a spin Hamiltonian, completely misses this aspect of metal physics. In general for nanoparticles containing a few thousand atoms, both types of excitations are present in the low-energy quantum spectrum of transition metal ferromagnetic nanoparticles.

Recently the low-energy quantum states of individual ferromagnetic metal nanoparticles have been directly probed by means of single-electron-transistor (SET) spectroscopy[17, 18, 19]. These experiments have indeed demonstrated the existence of a complex pattern of excitation spectra and spurred the elaboration of adequate theoretical models[20, 21, 22, 23] that include particle-hole and collective excitations on the same footing. It is clear that the quasiparticle states will change when the collective magnetization orientation is manipulated with an external field. Thus itinerant quasiparticle excitations can give rise to dissipation in the dynamics of the collective magnetization[24]. These important and interesting features represent a considerable complication that cannot be avoided in a theoretical treatment of macroscopic QTM in ferromagnetic metal nanoparticles. Dissipation from particle-hole excitations might be one of the reasons why preliminary experiments[5] on 3 nm Fe nanoparticles with $S \approx 800$ yield broad switching-field distribution widths that completely smear the expected field-separation steps coming from level quantization. There is, however, a regime where the quantum description of small transition metal clusters simplifies considerably, and their low-energy physics can be described by an effective Hamiltonian with a single giant spin degree of freedom, like that of a molecular magnet. Indeed, in Ref. 25 it was argued that a transition metal nanoparticle will behave like a molecular magnet when the energy scale associated with the collective magnetization, the magnetic anisotropy, is smaller than the typical energy scale associated with the quasiparticle degree of freedom, δ . This is the case for transition metal nanoparticles when the number of atoms is on the order of 100.

In this paper we study Landau-Zener macroscopic QTM in transition metal nanoparticles, in the regime where they behave like molecular magnets. In Ref. 25 it was shown

that in this case the total spin of the effective Hamiltonian describing the nanoparticle is specified by a Berry curvature Chern number that characterizes the topologically nontrivial dependence of the many-electron wavefunction on magnetization orientation. A prescription was given to derive microscopically the effective spin Hamiltonian by integrating out the quasiparticle degrees of freedom in the quantum action constructed within an approximate spin-density-functional theory framework. Here, however, we take a more pragmatic view, and we assume that the effect of the quasiparticle degrees of freedom, when integrated out, is to reshuffle randomly the pattern of avoided crossing gaps in the excitation spectrum of the collective-magnetization orientation degree of freedom used to describe uniaxial molecular magnets. Although this procedure might appear *ad hoc*, we believe that such a “random matrix theory” should capture part of the complicated interleaved excitation spectra in real systems, including those features due to surface-imperfections-induced randomness that are likely to be important in these very small grains. Our goal is to examine the effect of this randomness on the coherent macroscopic quantum transitions triggered by a magnetic field swept in the direction of the magnetization. We neglect in the present analysis every effect arising from decoherence and dissipation. We find different time evolutions depending on the presence or absence of disorder *and* on the initial conditions of the system. In the absence of disorder, if the initial state is close to the ground state, the system undergoes a few coherent transitions, corresponding to macroscopic tunneling of the collective spin between quasi-degenerate states. The asymptotic transition probability displays a small number of discrete peaks, with one dominant contribution. In general we find that the shift of the magnetization associated with the dominant transition is not large but still significant. A spectacular effect takes place if the system is prepared initially in a state of high-energy. In this case, during its time evolution, the system displays complete magnetization inversion, through a peculiar phenomenon that we call “backward cascade”. When disorder is added in the form of a random static transverse field, the average transition probability for a low-energy initial state acquires a continuous lineshape. Although the dominant delta-like peak found in the ordered case is now absent, the distribution is still sharply peaked around one of the transitions present before. Therefore we conclude that in this case disorder does not obliterate the occurrence of sharp features in the transition probability distribution that could be important for the observability of macroscopic quantum coherence. On the other hand, disorder may suppress the backward cascade effect occurring in the ordered case when

the initial state is a highly excited state. In this case at the end of the time evolution, the original wavepacket is spread essentially over all the eigenstates of the system.

The paper is organized as follows. In Sec. II we introduce a giant spin model describing a transition-metal nanoparticle in the molecular-magnet limit, and we illustrate some of its spectral properties. In Sec. III we discuss some paradigmatic features of the dynamical evolution of the collective magnetization under the effect of a time-dependent magnetic field. Disorder-averaged evolution of magnetization from the point of view of quantum diffusion is discussed in Sec. IV. In Sec. V we interpret our results in the context of a simplified network model, which offers an intuitive and possibly more generic picture of the magnetization reversal problem. Our conclusions are presented in Sec. VI, where we comment on the relevance of this work for the observation of QTM in ultrasmall ferromagnetic metal grains.

II. GIANT-SPIN MODEL FOR A FERROMAGNETIC METAL GRAIN

We consider an effective “spin” Hamiltonian aimed at modeling a ferromagnetic transition metal nanoparticle containing on the order of $N_a \approx 100$ atoms, in such a way that the total anisotropy energy KN_a is smaller than the single-particle mean-level spacing. Here K is the bulk anisotropy energy/atom. In this regime the nanoparticle behaves like a molecular magnet described by a collective quantum “spin” degree of freedom, $\hat{\mathbf{S}}$ [46]. It is important to emphasize that this collective “spin” is an effective variable representing coupled quasiparticle spin *and* orbital degrees of freedom of the original electron system. This coupling is non-trivial when spin-orbit interaction is included. The “spin” S can be specified by a Berry curvature Chern number that characterizes the topologically nontrivial dependence of the many-electron wavefunction on magnetization orientation[25]. The model that we consider has a uniaxial anisotropy term, augmented by a “transverse magnetic field”, which can be randomly distributed to mimic the combined remnant effect of quasiparticle excitations and structural disorder on the gap structure of the spin collective modes[47]. We will use matrix representations of the (dimensionless) operators $(\hat{S}_x, \hat{S}_y, \hat{S}_z)$ in the basis of the eigenstates $\{|S, m\rangle, -S \leq m \leq S\}$ of (\hat{S}^2, \hat{S}_z) , where z is aligned along the easy axis. The components of the “transverse field” are

$$\langle S, m | \hat{B}_x | S, m' \rangle = \delta_{m,m'} r_x(m) \Delta_x; \quad \langle S, m | \hat{B}_y | S, m' \rangle = \delta_{m,m'} r_y(m) \Delta_y. \quad (1)$$

Here Δ_x , Δ_y are given amplitudes, with dimensions of energy, and $r_x(m)$, $r_y(m)$ are uniformly distributed dimensionless random variables having width 1/2 and zero average. The resulting random coupling is described by the symmetrized operators

$$(\hat{B}_k \hat{S}_k)_{(R)} = (1/2)(\hat{B}_k \hat{S}_k + \hat{S}_k \hat{B}_k), \quad k = x, y, \quad (2)$$

having matrix elements:

$$\langle S, m | (\hat{B}_k \hat{S}_k)_{(R)} | S, m - 1 \rangle = i^{\epsilon(k)} \Delta_k (1/2) r'_k(m) [(S + m)(S - m + 1)]^{1/2}, \quad (3)$$

where $r'_k(m) = [r_k(m) + r_k(m - 1)]/2$ and $\epsilon(k) = 0, 1 (k = x, y)$. The effective spin Hamiltonian is then:

$$\hat{H} = -B_z(t) \hat{S}_z - K \hat{S}_z^2 - (\hat{B}_x \hat{S}_x)_{(R)} - (\hat{B}_y \hat{S}_y)_{(R)}, \quad (4)$$

where K is an effective anisotropy energy/spin. In Eq. (4) we have introduced the coupling to a time-dependent longitudinal field $B_z(t)$, which we will use to manipulate the collective spin spectrum and induce Landau-Zener type transitions at its avoided-crossing gaps. It is trivial to verify that \hat{S}^2 commutes with the operators in Eq. (2) and therefore the Hamiltonian of Eq. (4) remains within a given spin multiplet S . The size of the Hilbert space is $2S + 1$ and we will label the energy levels $E(m, t)$ with the discrete index m , running from $-S$ to S . We discuss some properties of the spectrum when $B_z(t)$ is linearly dependent on time: $B_z(t) = gt$. In Fig. 1 we plot the energy levels $E(m, t)$ as a function of time, for a generic disorder realization of the Hamiltonian given in Eq. (4) when $S = 50$. (The values of the other parameters of the Hamiltonian are specified in Sec. III.) It turns out that the density of states is higher in the upper part of the spectrum; the avoided crossings there predominantly involve channels associated with nearby sites along the m -chain. At lower energies the crossings involve channels associated with distant sites m , m' and the gaps are accordingly much smaller, as one can see by simple perturbative arguments. To lowest order the coupling is the product of l nearest neighbor amplitudes ($l = |m' - m|$). These features are clearly visible in Fig. 1. It was argued [21] that the peculiar diamond-like structure of the spectrum can be a signature of ferromagnetic metals. One can further notice that in the presence of a constant transverse magnetic field the nearest neighbor amplitudes favor backward (forward) motion in the region $m < 0$, ($m > 0$). This is due to the angular momentum matrix elements: the amplitude of the process $m \rightarrow m - 1$ is larger than the one relative to $m \rightarrow m + 1$ for $m < 0$, the asymmetry becoming stronger as m approaches

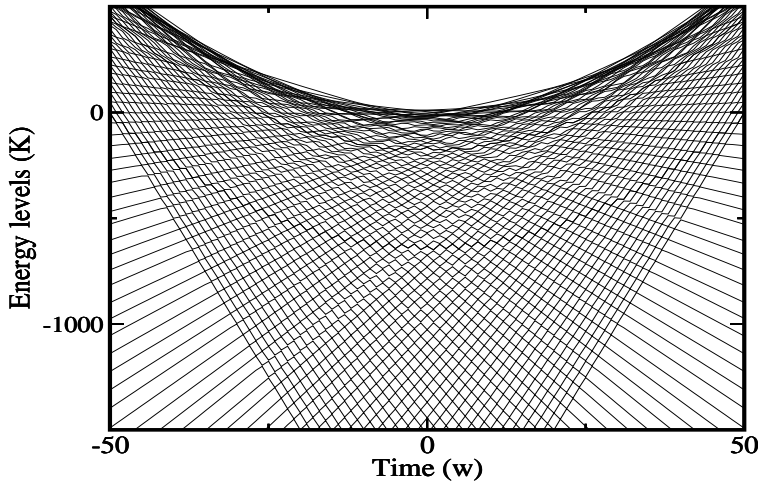


FIG. 1: Energy levels $E(m, t)$ vs. time of the random spin Hamiltonian defined in Eq.4, with total spin $S = 50$. The time unit is $w \simeq K/\hbar$, where K is the anisotropy energy/spin.

the ground state. In the classical limit $S \gg 1$ one has a potential barrier separating the two extremal states $m = \pm S$ [9].

III. SPIN DYNAMICS

The deterministic evolution of spin systems under the action of a time-dependent bias has been considered by various authors, mainly in the context of molecular magnets. Different situations have been considered, ranging from the case of a large, conserved spin multiplet S , to that of a general system of interacting spins [26, 27, 28]. The Landau-Zener theory provides a natural background for this class of problems [29, 30, 31]. The effect of noise on the Landau-Zener transitions has also been examined at length, in order to obtain a better understanding of the influence of the phonon and spin baths on macroscopic quantum coherence[33, 34, 35]. Here, the time evolution of a giant spin with time-independent disorder is supposed to represent the coherent dynamics of the magnetic moment of a monodomain ferromagnetic metal nanoparticle in a regime characterized by a large energy gap between the single-particle excitations and the collective “spin” modes. Our analysis will focus on the effect of quenched disorder.

The wave function $|\Psi(t)\rangle$ satisfies the time-dependent Schrödinger equation:

$$i\hbar \frac{d|\Psi(t)\rangle}{dt} = \hat{H}(t)|\Psi(t)\rangle \quad (5)$$

By expanding $|\Psi(t)\rangle = \sum_m c_m(t)|S, m\rangle$ on the basis $\{|S, m\rangle\}$, we obtain the following set of coupled differential equations for the coefficients $c_m(t)$

$$\begin{aligned} i\hbar \dot{c}_m(t) &= (-gtm - Km^2)c_m(t) \\ &- [(\Delta_x/2)r'_x(m) + i(\Delta_y/2)r'_y(m)][(S+m)(S-m+1)]^{1/2}c_{m-1}(t) \\ &- [(\Delta_x/2)r'_x(m+1) + i(\Delta_y/2)r'_y(m+1)][(S-m)(S+m+1)]^{1/2}c_{m+1}(t). \end{aligned} \quad (6)$$

The Schrödinger equation is integrated over a time interval $-T < t < +T$ such that at its extrema $t = \pm T$ the eigenvalues $E(m, t)$ are well separated: the diagonal part of the Hamiltonian being linear in t , and the coupling with the transverse field being bounded, the eigenvalues approach $-gtm$ for large enough $|t|$. More specifically, under the condition $|\Delta_x|, |\Delta_y| \ll S$, it is sufficient to fix the value of T as follows: $T > 4(KS)/g$. The eigenvalues then identify isolated channels and the time evolution can be studied as a scattering problem. In the present case, the ground state at $t = -T$ is $m = -S$ and turns into $m = +S$ at $t = +T$. One would like to integrate the Schrödinger equation over the interval $(-T, +T)$, with S on the order of 50 and realistic values of the other parameters, such as an anisotropy energy/spin on the order of $10^{-4}eV$, and a velocity of the bias $B_z(t)$ on the order of mTesla/sec. It is readily verified that this requires astronomical computation times. The situation is worse if one needs averaging over a large set of disordered configurations. We would like to emphasize here that in solving the time dependent Schrödinger equation, we don't want to make the frequently used approximation of reducing the full Hamiltonian into an effective two-level model. While this procedure is perhaps a justified approximation in the case of simpler models describing molecular magnets with small spins, the level intricacies present in our spectrum, which are at the heart of the problem we want to study, make this approximation completely meaningless.

As an example, we studied the case of the evolution from the channel $m = -46$, close to the ground state, with $K = 10^{-4}eV$ and $\Delta_x/\mu_B = \Delta_y/\mu_B = 0.02$ Tesla, μ_B being the Bohr magneton. In a series of runs we progressively reduced the sweep velocity down to 1 Tesla per second. Further examination of this case for, say, a sweep velocity of 10^{-1} Tesla per second requires a few days of computation time. At 1 Tesla per second, we obtained

that the system hops from $m = -46$ to $m = -43$. The question arises then: what can one expect at smaller sweep velocities? Could one obtain a much larger hopping range at, say, 1 mTesla per second? The Landau-Zener theory gives a negative answer to this question and a way out of the computation time problem. Let $\Delta_{\text{eff}}(m, m')$ be the (time-dependent) gap between two channels m, m' ; as long as this gap is reasonably large, wave packets carrying quantum numbers m and m' practically do not interfere. In the small transient at the crossing time (where the gap reaches a minimum) the two channels do interfere, and their scattering is determined by the Landau-Zener matrix $S(m, m')$ [36]. As is well known, the transition probability $P(m \rightarrow m')$ depends on the adimensional parameter $\nu(m, m') = [\Delta_{\text{eff}}(m, m')]^2 / (g\hbar|m - m'|)$:

$$P(m \rightarrow m') = 1 - \exp[-\pi\nu(m, m')/2]. \quad (7)$$

Notice that g scales as the square of the gap. Since, as already noticed, the gap corresponding to an hopping event of range l scales as the l -th power of a perturbative parameter, it is clear that upon reducing g by few orders of magnitude one will not detect hoppings of significantly larger range. This answers the question we made above. On the other hand, one can exploit the scaling between the gap and the sweep velocity in order to infer the behavior in the physical region from the results corresponding to numerically affordable values of the parameters. In a sequence of runs, we detected the transitions $m \rightarrow m + 1$, $m \rightarrow m + 2$, $m \rightarrow m + 3$, and so on. We then compared the crossing times resulting from time integration with the ones extracted by direct inspection of the spectrum $E(m, t)$, and found full agreement. As the crossing behavior appears to be scale invariant, one can argue that indeed the dynamics can be described as a sequence of L-Z transitions. This argument works provided that the hopping events involve two channels at a time. In the upper part of the spectrum, in particular in a region around $t = 0$, the channels are always close in energy and tend to hybridize. The resulting motion is a sequence of short range hoppings, as we will discuss in the sequel.

Based on the above considerations, in the remaining part of this Section we will consider a value for the sweeping speed that yields reasonable calculation times, although it lies beyond the experimentally meaningful range. Specifically, we introduce the time unit

$$w = \hbar/K, \quad (8)$$

where the anisotropy energy K will be taken as our energy unit. The sweeping speed is chosen in such a way that $g \cdot w^2/\hbar \approx 1$. As for the values of the transverse amplitudes, we will take $\Delta_x = \Delta_y \approx 2K$; an accurate estimate of these parameters should be based on microscopic derivations similar to the one suggested in Ref. [25], which is a task beyond the goal of this work. Our choice here is an educated guess based on the fact that if the gaps of the collective modes of a ferromagnetic metal nanoparticle are due in part to their coupling with quasi-particle excitations, in the regime where the mean-level spacing of the latter is larger than the total anisotropy energy, the values of the fictitious transverse field should lie within a range not smaller than K . Below we discuss the time evolution of the system both in the disordered and ordered case. In the ordered case the values of the transverse field B_x^0 , B_y^0 have been chosen equal to the mean square roots of the random amplitudes: $B_x^0 = (\langle B_x^2 \rangle)^{1/2} = \Delta_x / (2 \cdot 3^{1/2}) \approx \Delta_x \cdot 0.28867$.

We start by examining two paradigmatic behaviors enabling to reconstruct the generic case. The first is found when the initial state is in the low energy region $m \geq -50$. Generally the system undergoes a major hopping event toward a channel $m' > m$, but the hopping range $l = m' - m$, even if significant, is always far from what one would need for magnetic inversion. This is clearly due to the presence of gaps of almost insurmountable smallness: these, as it is well known, do occur in the ordered case as well. It must be recalled that magnetic inversion in molecular magnets, in spite of a smaller spin, is generally observed with the essential contribution of relaxation and decoherence processes, which are not taken into account here. From our results it appears that in general the disorder reduces the size of the gaps: more precisely some of the gaps that in the ordered case are large enough to give rise to hopping, with disorder are no longer “seen”, so that the state keeps its quantum number. We also found that as the initial channel m , ($m < 0$) is closer to the ground state, the hopping range becomes shorter. The reason for this has been discussed in Section II. In Fig. 2 we plot the probability distribution

$$P(m, t) \equiv |\langle S, m | \Psi(t) \rangle|^2 \quad (9)$$

as a function of time and channel index m , for the disordered [Fig. 2(a)] and the ordered [Fig. 2(b)] case, respectively. Only one disorder realization is considered here. In both cases the initial wavefunction $|\Psi(t = -T)\rangle$ is a state of sharp z -component of the collective spin, taken in the low-energy part of the spectrum (eigenvalue index $m = -25$), where the

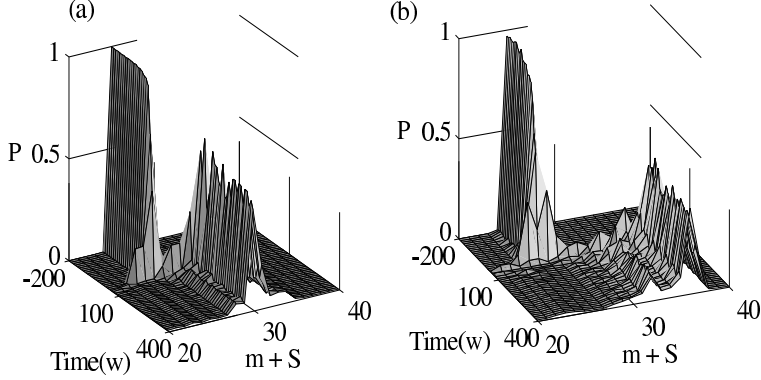


FIG. 2: Probability distribution $P(m, t) \equiv |c_m(t)|^2 = |\langle S, m | \Psi(t) \rangle|^2$ as a function of time and the index m . The initial wavefunction is prepared in a state of low energy, $m + S = 25$. (a) Random case. (b) Deterministic case.

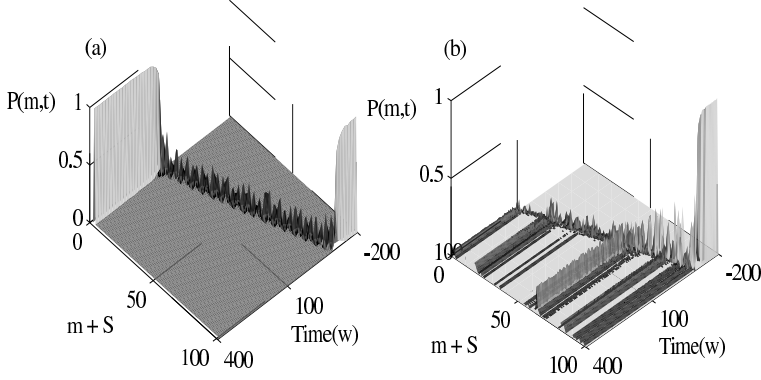


FIG. 3: The same as in Fig. 2 but for an initial wavefunction prepared in an excited state of high energy, $m + S = 100$. (a) Deterministic case. (b) Random case.

magnetization $\langle \hat{S}_z \rangle$ is large and negative. As shown in Fig. 2(a), in the disordered case the system undergoes a single major hopping event at large positive times. The result is a rather small magnetization shift $\Delta \hat{S}_z = \langle \hat{S}_z(+T) \rangle - \langle \hat{S}_z(-T) \rangle$, smaller than what one observes in the deterministic case, shown in Fig. 2(b).

In order to better see how this transition comes about, in Fig. 4 we plot, as a function of time, the part of the spectrum blown up around the region where the quantum tunneling for the disordered case described in Fig. [2](a) occurs. The gray (red in color version) bold line moving up-right represents the time evolution of the energy of the initial state, labeled by $m + S = 25$. As shown in the figure, at time $t \approx 20w$, the level starts to encounter large gaps. The first transition is a jump down into a state of lower m ; at $t \approx 25w$, the level

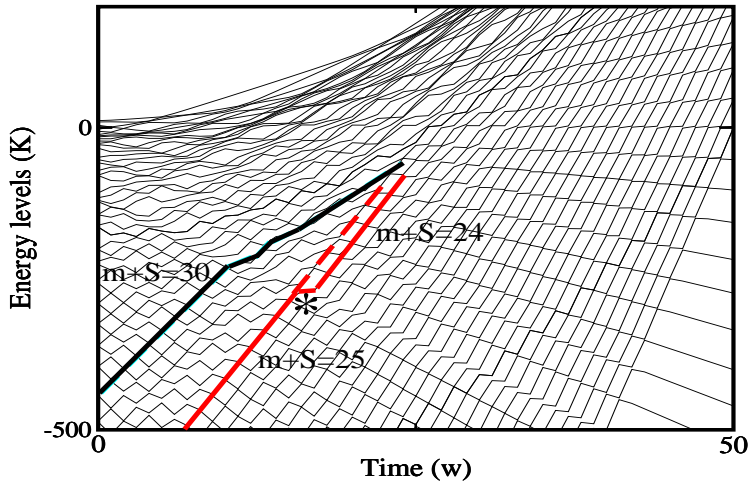


FIG. 4: Energy levels vs. time as in Fig. 1. The spectrum as been blown up in the region corresponding to the initial phases of the quantum tunneling described in Fig. [2](a). The gray (red in color version) bold line represents the time evolution of the energy of a quantum state initially prepared in $m + S = 25$. At $t \approx 20w$ (where the asterisk is) the state first jumps into the state $m + S = 24$. Then it starts merging, at $t \approx 25w$, with a narrow group of states centered around the state with $m + S = 30$ (black bold line), which are also moving up and bending toward the right.

starts merging with a group of states sharply centered around level $m + S = 30$ (represented by the black bold line), which are also moving up and bending toward the right. If one starts at higher energies, yet still in the low-energy region ($\langle \hat{S}_z \rangle < 0$), another mechanism comes into play, associated with the second of the two announced behaviors, which we will call *backward cascading*. This process, particularly clear when the initial state is in the high-energy region, can be understood as follows. Every couple of channels m, m' is expected to undergo a crossing at the approximate time $t_{m,m'} = -K(m + m')/g$, obtained by equating the unperturbed energies : $E^0(m, t) = E^0(m', t)$, with $E^0(m, t) = -gtm - Km^2$. The exact crossing time, provided that the couplings Δ_x and Δ_y are small enough, will be perturbatively close to it. The nearest-neighbor level crossing ($m \rightarrow m' = m \pm 1$) occurs approximately at the time $t_m \approx (-2Km)/g$: the very fact that t_m is a decreasing function of m is at the origin of the backward cascading process. In fact, if the system hops from m to a higher value m' , since $t(m') < t(m)$, it has no longer a chance to undergo a further

nearest-neighbor transition. If on the contrary $m' < m$, the next hopping time has still to come, so that backward motion can be iterated. One can then expect, upon starting from the highest energy state $m = S$, a ballistic backward motion ending at $m = -S$. This is in fact found in the deterministic case, as shown in Fig. 3(a). We have complete magnetic inversion, connecting energy maxima, similar to the pendulum kink, with no dispersion. The hopping terms in the Hamiltonian drive the wave packet down from the local maximum along the energy profile, but the ballistic velocity equals the time variation of the energy, so that the wave packet stays on the maximum. Disorder inhibits the coherent sequence of nearest neighbor hoppings; portions of the wavepacket are then trapped at intermediate channels; the result is a damped backward avalanche, undergoing fragmentations along the way. Accordingly, the final variance is extremely large, and complete magnetic inversion is frustrated, as shown in Fig. 3(b).

In conclusion, when the initial state of the system is in the low-energy region, the main feature of its time-evolution is the quantum tunneling of the collective spin, associated with a small but not negligible shift of the magnetization. When the system starts from an highly excited state, the backward cascading is the salient event of the dynamics. The time evolution of the magnetic system when starting from a generic state appears to be a combination of the two behaviors described above.

IV. DISORDER-AVERAGED TRANSITION PROBABILITY

So far we illustrated data originating from single samples. We will now discuss the disorder-averaged transition probability from the initial state m to the final state m' , defined as

$$\langle\langle g_{m',m} \rangle\rangle = \langle\langle |\langle m' | U(+T; -T) | m \rangle|^2 \rangle\rangle.$$

Here, with obvious notation, $U(t'; t)$ is the evolution operator from t to t' and the double bracket denotes the ensemble average. In Fig. 5 we plot $\langle\langle g_{m',m} \rangle\rangle$ (black solid lines) for the initial conditions (a)-(d) marked by the vertical dashed lines. The function $g_{m',m}$ for the corresponding deterministic case (gray solid lines—red in color version), with the same initial conditions, is also plotted for comparison. The disorder-averaged probability displays a single broad peak at a value $m_{max} = m_{max}(m)$, a smooth decay in the region $m' < m_{max}$ and a very steep decay on the opposite side of the peak. One can notice that

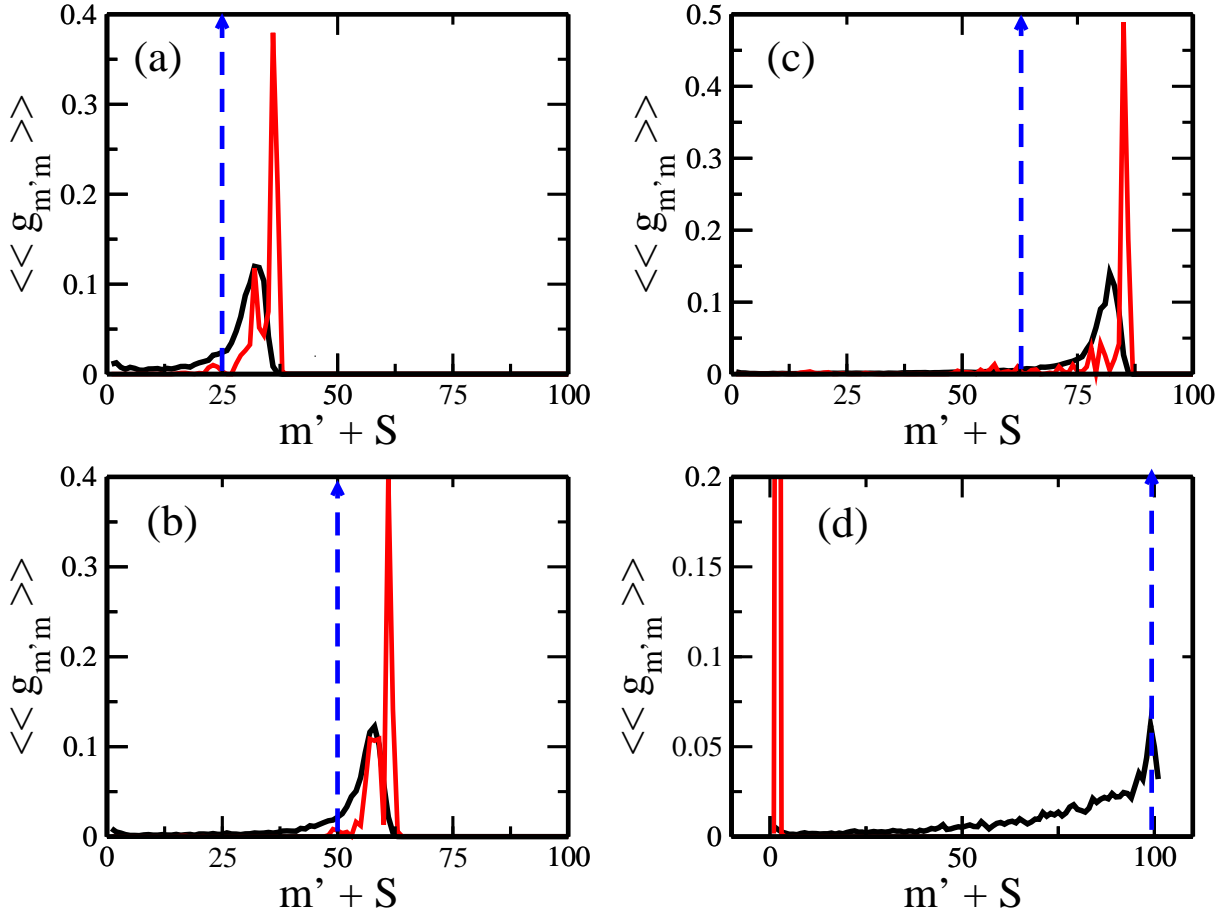


FIG. 5: Disorder-averaged transition probability $\langle\langle g_{m',m} \rangle\rangle$ (black solid lines). For comparison, the transition probability $g_{m',m}$ for the deterministic case (gray solid lines—red in color version) is also included. (a)-(d) represent four different initial conditions. The vertical dashed line marks the spin quantum number m of the initial state. Note in (d) the complete “backward cascade” behavior, which turns into a “cascade with traps” in the disordered case.

$m_{max} > m$, so that it can be identified with the main hopping event discussed above. The sensitive asymmetry of the distribution can be explained in terms of the time ordering of the scattering times: in fact, after the main hopping event has taken place, the backward cascading is definitely favored with respect to further forward hoppings. We also determined the disorder-averaged variance of S_z as a function of time

$$\langle\langle (\Delta S_z)^2 \rangle\rangle \equiv \langle\langle \langle \Psi(t) | (S_z - \langle S_z \rangle)^2 | \Psi(t) \rangle \rangle \rangle \quad (10)$$

for various initial conditions. This is shown in Fig. 6.

In summary, when starting from low energy channels (see Fig. 6(a)) there is a peak at the

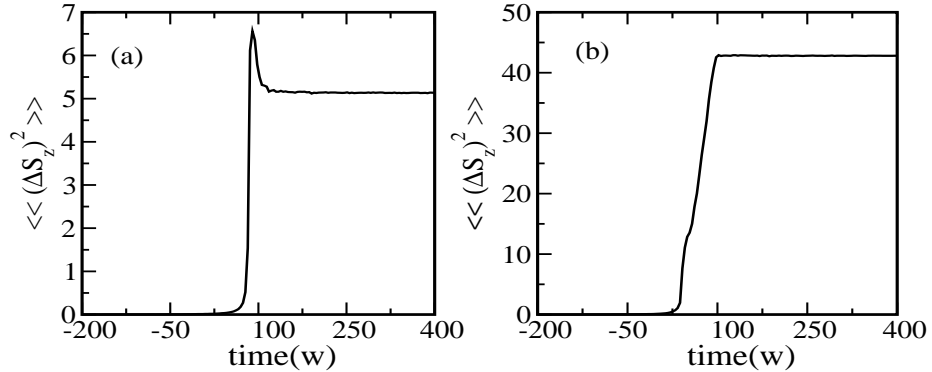


FIG. 6: Variance of $S_z(t)$ averaged over disorder, as a function of time. (a) Initial state of low energy ($m + S = 5$); (b) initial state of higher energy ($m + S = 25$).

hopping event, then the function rapidly decays to a constant value: in fact during the main transition to m_{max} , portions of the wave packet undergo hoppings of shorter range, and no longer move afterwards. The picture changes when the initial state has higher energy (see Fig. 6(b)): then, following the main hopping event, a cascading process is always present. This process is a frustrated ballistic motion: the variance displays a linear time dependence, as in quantum diffusion, clearly visible in the time region laying between the initial transient and the final saturation. Notice that the saturation value is almost one order of magnitude larger than in case (a).

V. NETWORK OF LANDAU-ZENER CROSSINGS

We now give a qualitative interpretation of our results, in terms of a simple network model representing the time evolution of the energy levels. The nodes of the network are associated with the m, m' crossings. Coherently with this interpretation, we will use a terminology commonly employed in studying quantum transport in lattice models, when this is viewed as an inter-channel scattering problem described by the Landauer-Büttiker formalism. Landau-Zener grids were originally introduced in studying the incoherent mixing of Rydberg manifolds [37]. In the approach suggested below the coherent quantum evolu-

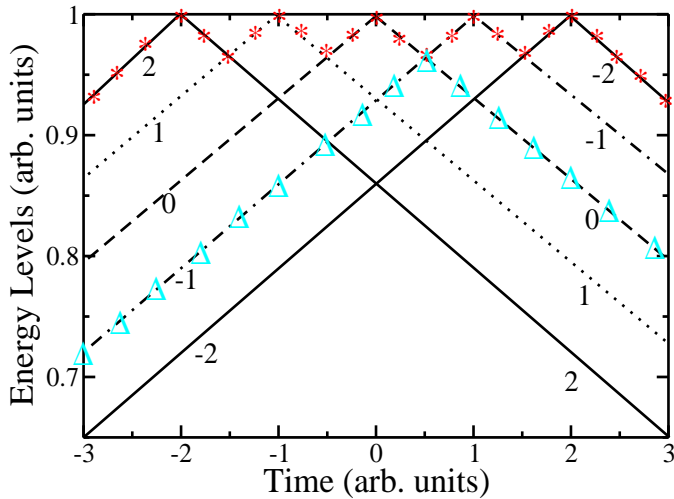


FIG. 7: Network model in the (t, E) plane, mimicking the time dependence of the level structure of Fig.1. The path marked by the triangles represents the evolution of the system undergoing quantum tunneling of the magnetization. The path marked by asterisks represents backward cascade evolution that occurs when the system starts from a high-energy state.

tion is instead taken into account. Due to the presence of the ferromagnetic S_z^2 term in the Hamiltonian, the present network has a peculiar topology, which can be schematically represented as a family of parallel lines in the presence of a boundary acting as a mirror plane. We display this network in Fig. 1, where the energies are plotted as a function of time. All the lines are equally oriented with increasing times; in the simplest situation the avoided crossings involve no more than two lines at a time, although, as stated in Sec. III, the detailed structure of the spectrum is much more complicated than this and deserves particular care. A simplified version of this pattern is a lattice where the crossing times are fixed at their unperturbed values $t_{m,m'} = -K(m + m')/g$, as depicted in Fig. 7. Using an optics analogy, each lattice node acts as a beam splitter, where the field amplitude transmission corresponds to channel conservation ($m \rightarrow m$) and the reflection to inter-channel hopping ($m \rightarrow m'$). At the turning points laying on the horizontal line ($E = 1$) the channel is conserved. The time coordinate is oriented from left to right, as in Fig. 1. The transfer matrix \mathcal{T} for the network of Fig. 7 is the time-ordered product of single step matrices acting on the space of wave functions c_m . It is convenient to enumerate the channels with the index

$n = m + S + 1$, ($n = 1, N; N = 2 \cdot S + 1$). A generic single step matrix, labeled by the “scattering time” index k , ($k = 3, 2 \cdot N - 1$), is the product of Landau-Zener $U(2)$ operators, one for each crossing ($n \rightarrow n'$) occurring at time k . The crossings are determined by the equation $n + n' = k$; ($0 < n < n' \leq k$).

Let us discuss the deterministic case first. One easily realizes that as the distance from the “mirror” line increases, the hopping probability decreases; in fact this distance goes as $|m - m'|$, hence nodes laying far from the “mirror” line involve long range hoppings and small gaps, i.e. small Landau-Zener hopping probabilities. The network can be separated in two regions, respectively dominated by channel conservation (i.e. localization) and by hopping (i.e. delocalization). The boundary between the two regions, i.e. the ideal curve where the hopping probability is $1/2$, is approximately parallel to the “mirror” line. It is natural to call this boundary “mobility curve”, although it is not a mobility edge in the usual sense. If, e.g., the particle is initially in the upper energy level, it never leaves the delocalized region: its most probable path is a sequence of nearest neighbor hoppings, ending in the final upper level. This explains the ballistic backward cascade. This type of time evolution is represented schematically on Fig. 7 by the path labeled by asterisks. When starting from a low energy state, the particle first propagates in the localized region; at some time it will cross the mobility curve and only at this point it will start hopping, giving rise typically to one quantum tunneling event only. This second time evolution is marked on Fig. 7 by the path of triangles. The above analysis can be extended to the disordered case. One can expect that the boundary between localized and delocalized regions has then a rather intricate shape; furthermore, since disorder on average lowers the number of “large gaps” the delocalized region accordingly reduces its size. The backwards ballistic motion described above is possible provided that a delocalized strip of almost constant width exists. If the mobility “curve” undergoes fluctuations, and on average approaches the mirror line, at the narrowings of the delocalized strip some portions of the wave packet must enter the localized region. The result is a frustrated motion, where various portions of the wave packet get trapped at intermediate states. If the particle starts evolving from a low energy channel, its representative line will reach the mobility curve at a later time as compared with the deterministic case: this also implies a smaller range $|m - m'|$ of the main hopping event $m \rightarrow m'$, ($m' > m$). The plots of the transition probability, exhibited in Fig. 5 are consistent with this description; qualitatively the peaks of these plots identify the average

location of the mobility boundary.

VI. CONCLUSIONS

In this article we have investigated the occurrence of Landau-Zener macroscopic quantum tunneling of the magnetization in a giant-spin model ($S = 50$) in the presence of random anisotropy. The model is intended to provide a phenomenological description of the low-energy spin dynamics of a ultra-small ferromagnetic metal nanograin, in a regime where the quasi-particle mean level spacing is larger than the total anisotropy energy and the metal grain behaves like a molecular magnet. We have focused, in particular, on the effects of the disorder on the gap structure of the spin collective modes. The microscopic origin of this randomness is ultimately related to the non-trivial physics of the itinerant quasiparticles of the underlaying electronic system.

We find that the time evolution of the system under the action of a Landau-Zener time-dependent magnetic field depends on the interplay between disorder and initial conditions. For a disorder-free model starting from a low-energy state, there is one main coherent quantum transition event, with a non-negligible shift in the magnetization. In correspondence of this transition the occupation amplitude of the original state is essentially totally depleted. The final (large-time) transition probability distribution is characterized by a few discrete peaks, with one dominant contribution. Disorder does not obliterate these signatures of macroscopic quantum coherence: the disorder-averaged transition probability distribution is smooth, sharply peaked and strongly asymmetric. The resulting shift in magnetization, at a sweep velocity of the order of mTesla/sec, is estimated in a few percents of the spin S . When the system is initially prepared in the high-energy excited state, it is subject to multiple tunneling giving rise to a ballistic motion ending in a final state with complete magnetization reversal. This curious coherent time evolution is made possible by the hopping probability being equal to one during the whole process. On the other hand, when disorder is present, at each step the wave packet finds a non zero probability of being trapped: as a result the amplitude of the ballistic wave packet gets damped along the way.

Our results provide some indications about the observability of macroscopic quantum coherence in ferromagnetic nanoparticles containing approximately 100 atoms. Specifically the sharp features in the transition probability, which are robust against disorder, can perhaps

be observed in detailed Landau-Zener SQUID magnetometry experiments on single particles or ensemble of particles, similar to the ones performed by Wernsdorfer and colleagues[5, 16].

The scenario presented above excludes macroscopic magnetic inversion at affordably slow sweep velocities, as well as hysteresis; by considering decoherence i.e. the decay of the non diagonal elements of the density matrix, and dissipation, i.e. the damping of its diagonal part[32, 38], these effects should obviously come into play. In the analysis done in Ref. [39, 40], where the L-Z theory with one level crossing has been generalized to include decoherence and dissipation, it was found that the decoherence does not completely destroy the quantum nature of the evolution. The main features of the Landau-Zener model are thus preserved in the pure decoherence (non dissipative) case and survive to a limited amount of dissipation. For the large-spin system considered in this paper the Hamiltonian dynamics can be described in terms of a sequence of L-Z level crossings. An important remaining question which we have not investigated here is whether or not this picture survives in an open system. The problem of the non-Hamiltonian spin dynamics, already addressed in the past for small quantum spins (see below), is still the object of intense investigation.

A possible source of dephasing and dissipation is the coupling of the nanoparticle magnetic moment to a particle-hole continuum, such as a metallic substrate and the electron system of the particle itself. As we have explained above, the latter should not be important in the molecular magnet regime that we have considered in this work. The coupling to the substrate, on the other hand, can be controlled by changing the thickness of the insulating barrier between the nanoparticle and substrate.

Another cause of decoherence comes from the coupling to the phonon bath. Interestingly enough, the possibility of controlling part of phonon-induced phenomena has been demonstrated in the case of the low-spin molecular system V_{15} [41]

At low temperatures the dominant cause of decoherence arises from the unavoidable coupling to nuclear spins. The central spin model considered in Ref. 42, where the microsystem is a single $S = 1/2$ spin, is the best known description of the spin bath effects; within that theory, deviations from the Landau-Zener behavior have been pointed out [35]. An analysis of spin bath effects on metallic ferromagnetic nanoparticles goes beyond the scope of the present work. We recognize that the coupling to nuclear spin baths can considerably affect the macroscopic quantum coherence studied here. It is reasonable to assume that this coupling can influence to a larger degree the decoherence rather than the dissipation, since

the phases of the macroscopic spin are sensitive to the nuclear spin precessions, while its energies are merely perturbed by the spin bath.

As mentioned in the introduction, so far the only experimental attempts to detect directly MQT in single ferromagnetic nanoparticles has been done by Wernsdorfer *et al.*[5, 16] through magnetization measurements. An idea that we would like to propose here is to search for evidence of MQT in transport experiments on magnetic SETs similar to the ones performed by D. Ralph's group[17, 18], but in the presence of a L-Z time-dependent field[48]. In SET experiments with a magnetic nanoparticle as the central island, the coupling between the nanoparticle electronic states and its magnetic moment causes abrupt changes in the energy of conductance resonances at the classical switching field. This effect was investigated theoretically in recent papers[22, 43]. An interesting question to ask is how the coherent QTM between two degenerate quantum states affects the conductance. From the analysis carried out in this work, we know that for a large spin ($S \approx 100$) MQT might be observable only at fields close to the classical switching field. Thus SET transport experiments should give us a clear landmark of the surroundings of where MQT should be looked for. How macroscopic quantum coherence would affect the tunneling resonances is however not obvious and deserves to be further investigated. Conversely, if MQT in single magnetic particles could be detected by means of ordinary magnetization measurements, one very interesting question is to what extent current flow will influence dephasing of the magnetic macroscopic quantum coherence. Work along these lines is presently underway[49]. As for the coupling of the nanoparticle to a metallic substrate, the level of decoherence and dissipation coming from the tunneling current might be controlled by changing the tunnel barriers of the SET.

VII. ACKNOWLEDGMENTS

We would like to thank W. Wernsdorfer, D. Ralph and A. H. MacDonald for interesting discussions. This work was supported in part by the Swedish Research Council under Grant No:621-2001-2357 and by the Faculty of Natural Science of Kalmar University. Support from the Office of Naval Research under Grant N00014-02-1-0813 is also gratefully acknowledged.

[1] I. M. L. Billas, A. Châtelain, and W. A. de Heer, *Science* **265**, 1682 (1994).

- [2] M. Lederman, S. Shultz, and M. Ozachi, Phys. Rev. Lett. **73**, 1986 (1994).
- [3] R. H. Kodama, J. Magn. Magn. Mater. **200**, 359 (1999).
- [4] R. Sessoli, D. Gatteschi, A. Caneschi, and M. A. Novak, Nature **365**, 141 (1993).
- [5] W. Wernsdorfer, Adv. Chem. Phys. **118**, 99 (2001).
- [6] S. A. Majetich and Y. Jin, Science **284**, 470 (1999).
- [7] S. Sun, C. B. Murray, D. Weller, L. Folks, and A. Moser, Science **287**, 1989 (2000).
- [8] M. Jamet, W. Wernsdorfer, C. Thirion, D. Mailly, V. Dupuis, P. Mélinon, and A. Péres, Phys. Rev. Lett. **86**, 4676 (2001).
- [9] A. Garg, cond-mat/0012157.
- [10] L. Gunther and B. Barbara, eds., *Quantum Tunneling of Magnetization*, QTM94 (Kluwer, Dordrecht, 1995).
- [11] E. Chudnovsky and J. Tejada, *Macroscopic Quantum Tunneling of the Magnetic Moment* (Cambridge University Press, Cambridge, 1998).
- [12] L. Thomas, F. Lioni, R. Ballou, D. Gatteschi, R. Sessoli, and B. Barbara, Nature **383**, 145 (1996).
- [13] J. R. Friedman, M. P. Sarachik, and J. Tejada, Phys. Rev. Lett. **76**, 3830 (1996).
- [14] C. Sangregorio, T. Ohm, C. Paulsen, R. Sessoli, and D. Gatteschi, Phys. Rev. Lett. **78**, 4645 (1997).
- [15] W. Wernsdorfer and R. Sessoli, Science **284**, 133 (1999).
- [16] W. Wernsdorfer, E. B. Orozco, A. Benoit, D. Mailly, O. Kubo, H. Nakamo, and B. Barbara, Phys. Rev. Lett. **79**, 4014 (1997).
- [17] S. Guéron, M. M. Deshmukh, E. B. Myers, and D. C. Ralph, Phys. Rev. Lett. **83**, 4148 (1999).
- [18] M. M. Deshmukh, S. Kleff, S. Guéron, E. Bonnet, A. N. Pasupathy, J. von Delft, and D. C. Ralph, Phys. Rev. Lett. **87**, 226801 (2001).
- [19] M. M. Deshmukh (2002), ph. D. thesis, Cornell University 2002.
<http://www.ccmr.cornell.edu/~mandar/mandar-thesis.ps.gz>.
- [20] C. M. Canali and A. H. MacDonald, Phys. Rev. Lett. **85**, 5623 (2000).
- [21] A. H. MacDonald and C. M. Canali, Solid State Comm. **119**, 253 (2001).
- [22] S. Kleff, J. von Delft, M. M. Deshmukh, and D. C. Ralph, Phys. Rev. B **64**, 220401 (2001).
- [23] A. Cehovin, C. M. Canali, and A. H. MacDonald, Phys. Rev. B **68**, 014423 (2003).
- [24] G. Tatara and H. Fufuyama, Phys. Rev. Lett. **72**, 772 (1994).

[25] C. M. Canali, A. Cehovin, and A. H. MacDonald, Phys. Rev. Lett. **91**, 046805 (2003).

[26] D. A. Garanin and R. Schilling, cond-mat/0307371.

[27] S. Miyashita and N. Nagaosa, cond-mat/0108063.

[28] D. A. Garanin, cond-mat/0302107.

[29] L. D. Landau, Phys. Z. Sowjetunion **2**, 46 (1932).

[30] C. Zener, Proc. Roy. Soc. Lond. A **137**, 696 (1932).

[31] E. C. G. Stückelberg, Helv. Phys. Acta **5**, 369 (1932).

[32] M. N. Leuenberger and D. Loss, cond-mat/9911065.

[33] K. Saito and Y. Kyanuma, cond-mat/0111420.

[34] V. L. Pokrovsky and S. Scheidl, cond-mat/0312202.

[35] N. A. Sinitsyn and N. Prokoféf, Phys Rev B **67**, 134403 (1997).

[36] V. Pokrovsky and N. Sinitsyn, cond-mat/0012303.

[37] D. A. Harmin and P. N. Price, Phys Rev A **49**, 1933 (1994).

[38] V. V. Dobrovitski, M. I. Katznelson, and B. N. Harmon, Phys. Rev. Lett **84**, 3458 (2000).

[39] V.G.Benza and G.Strini, quant-ph/0203110.

[40] V.G.Benza and G.Strini, Fortschr. Phys. **51**, 14 (2003).

[41] I. Chiorescu, W. Wernsdorfer, A. Müller, S. Miyashita, and B. Barbara, cond-mat/0212181.

[42] N. Prokoféf and P. Stamp, cond-mat/0001080.

[43] A. Cehovin, C. M. Canali, and A. H. MacDonald, Phys. Rev. B **66**, 094430 (2002).

[44] G.-H. Kim and T.-S. Kim, Phys. Rev. Lett. **92**, 137203 (2004).

[45] In discussing quantum tunneling phenomena involving macroscopic variables it is important to distinguish between *incoherent tunneling* of the system out of a classically metastable potential well and *coherent tunneling* between two classically degenerate minima separated by an impenetrable barrier[10]. In the second case, coherent tunneling removes the degeneracy of the two original ground states causing a level splitting. In this paper we will loosely use the expression macroscopic quantum tunneling to indicate macroscopic quantum coherence, that is coherent tunneling.

[46] When the bulk density of states is used to evaluate δ , one finds[25] that a transition metal nanoparticle will behave like a molecular magnet when $N_a < 120$ in Co and $N_a < 750$ in Fe.

[47] It is important to point out that this random Hamiltonian does not include the coupling of the nanoparticle magnetic moment with other types of excitations, e.g. the ones related to the

degrees of freedom of the nuclear spin bath. Such coupling is likely to be an important source of decoherence. We will comment on this point in Sec. VI.

- [48] While we were completing this work we became aware of a recent paper[44], where a similar suggestion for the study of MQT in *molecular magnets* was put forward.
- [49] D. Ralph, private communication.